

Article

Experimental Investigation of Communication Performance of Drones Used for Autonomous Car Track Tests

Melih Yildiz ^{1,*}, Burcu Bilgiç ², Utku Kale ³ and Dániel Rohács ³

¹ Department of Aeronautical Engineering, Faculty of Aviation and Space Sciences, Girne University, 99320 Mersin, Turkey

² Department of Electrical and Electronics Engineering, Atilim University, 06830 Ankara, Turkey; burcu.bilgic@atilim.edu.tr

³ Department of Aeronautics and Naval Architecture, Faculty of Transportation Engineering and Vehicle Engineering, Budapest University of Technology and Economics, 1111 Budapest, Hungary; ukale@vrht.bme.hu (U.K.); drohacs@vrht.bme.hu (D.R.)

* Correspondence: melih.yildiz@kyrenia.edu.tr

Abstract: Autonomous Vehicles (AVs) represent an emerging and disruptive technology that provides a great opportunity for future transport not only to have a positive social and environmental impact but also traffic safety. AV use in daily life has been extensively studied in the literature in various dimensions, however; it is time for AVs to go further which is another technological aspect of communication. Vehicle-to-Vehicle (V2V) technology is an emerging issue that is expected to be a mutual part of AVs and transportation safety in the near future. V2V is widely discussed by its deployment possibilities not only by means of communication, even to be used as an energy transfer medium. ZalaZONE Proving Ground is a 265-hectare high-tech test track for conventional, electric as well as connected, assisted, and automated vehicles. This paper investigates the use of drones for tracking the cars on the test track. The drones are planned to work as an uplink for the data collected by the onboard sensors of the car. The car is expected to communicate with the drone which is flying in coordination. For the communication 868 MHz is selected to be used between the car and the drone. The test is performed to simulate different flight altitudes of drones. The signal strength of the communication is analyzed, and a model is developed which can be used for the future planning of the test track applications.

Keywords: autonomous vehicles; V2V; car test data collection; connected vehicle; sustainability

Citation: Yildiz, M.; Bilgiç, B.; Kale, U.; Rohács, D. Experimental Investigation of Communication Performance of Drones Used for Autonomous Car Track Tests. *Sustainability* **2021**, *13*, 5602. <https://doi.org/10.3390/su13105602>

Academic Editor: Pan Lu

Received: 19 March 2021

Accepted: 13 May 2021

Published: 17 May 2021

Publisher's Note: MDPI stays neutral with regard to jurisdictional claims in published maps and institutional affiliations.



Copyright: © 2021 by the authors. Licensee MDPI, Basel, Switzerland. This article is an open access article distributed under the terms and conditions of the Creative Commons Attribution (CC BY) license (<http://creativecommons.org/licenses/by/4.0/>).

1. Introduction

Unmanned aerial vehicles (UAVs) are of great interest because of their wide range of application fields. Drones are UAVs that are equipped with sensors and communication devices. Besides their wide area of use, drones can improve vehicle-to-vehicle connectivity by cooperating with vehicles and collecting information. Drones can be used to cooperate in air-to-ground communication and to assist communication infrastructure where it is not available, or connectivity is poor [1].

Thanks to its easy deployment and low cost of ownership, UAVs draw interest for their integration into Vehicular Ad-hoc Networks (VANETs) [2]. Although the focus on drone integration studies is given to improving network connectivity, enhancing information collection ability, and intra-networking issues [3], a small number of studies proposed using drones in VANET networks. Using drones for communication relay between vehicle-to-vehicle (V2V) communications to decrease the average end-to-end packet delivery delay is studied [4].

Simulation results, which investigate the challenges and deployment opportunities of DAVNs (Drone Assisted Vehicular Networks), demonstrate that the performance of

vehicular networks can be significantly enhanced with the proposed DAVN architecture [3].

Zhou et al. built an air-to-ground vehicular communication network and validated its performance by road tests [5]. In this study, an aerial sub-network is formed by drones that assist the ground vehicular network. The drones used in this test for collecting data from vehicles and performing a relay for communication.

Oubbati et al. proposed a network in which drones are used to monitor traffic density and vehicle connectivity status, and then exchange collected information with vehicles through dedicated messages [6].

V2V communication is also widely analyzed for video surveillance function for traffic monitoring [7].

Specifically, the integration of drones and Vehicle Networks (VN) can bring the following benefits [3]:

- •Improving Reliability for Wireless Links
- •Enhanced significantly. Enhancing Flexibility for Infrastructures
- •Providing Connectivity for Resource-less Scenarios

The test tracks which have long ranges of the test field would require a high amount of infrastructure installation and operation. Using drones for data collection during a test can help to reduce the cost of infrastructure, particularly with autonomous tracking capability.

V2V offered as a wireless power transfer tool for extending the ranges and charging the batteries while on the move [8]. Research also gives an insight into the possibility of using V2V communication in energy harvesting as an energy supply [9]. In this study, the communication between low altitude drones following a car and car under test is analyzed. This research presents an experimental setup for radio signal analysis study of Air-to-Ground (A2G) drone communication at an operating frequency of 868 MHz. A series of measurements are performed over a range of 2 km, simulating low-altitude, car following drones with different distance, and altitude options. Simulations of the altitude of the drones are performed for 45 cm, 95 cm, and 165 cm using bars which resemble these altitudes, and the path losses on the communication between drone and car are performed for distances starting from 120 m up to 2 km. By analyzing the test data, the effect on the path loss of range and altitude at ambient conditions is studied. The experimental results for communication between low altitude drones and cars are used to develop a path loss considering the ground effect. In this research, small-scale damping is defined by Rician fading and the distance path loss model is derived.

To achieve the optimum performance out of drone operations, the altitude of the drone is very important. It is required to have high communication performance while providing the highest possible endurance. Although increasing the drone altitude increases the probability of Line of Sight (LoS) communication with the car under test [10], in case of following a single car on the track, the altitude of the drone shall be selected as close to the car as possible. The low altitude, in this case, will create a problem of ground effect on communication.

In this research, the ground effect on communication between autonomous cars under test and low altitude flying drones is studied. This study was conducted using an omnidirectional antenna. It is assumed that the drone is flying level and no inclination is considered. In the experimental setup, the relative speed between the drone and car is taken to be zero, assuming the drone is following the car at the same speed.

In order to increase battery energy efficiently, the use of low-frequency communication plays an important role. The ground effect on the communication thus analyzed by researchers at various frequencies such as VHF, UHF [11], 800–1800 MHz [12], 917.5 MHz [13], 433 MHz, and 2.4 GHz [14]. Power usage is critical, especially for off-grid machines with batteries, such as drones. It is even more important when drones are required to fly in a long-range and endurance with a limited battery capacity. The capacity

of the battery is limited by the payload capacity of the drone. The drone design process is an optimization process of the payload, range, and endurance parameters. The frequency of the communication deployed on the drone is another parameter that affects battery capacity and as a result other three parameters. Due to the wide coverage and ease of utilization using existing land wireless networks is preferred in general literature such as LTE [15], and WiFi [16], but as in most of the cases, it requires higher frequencies, it may not be feasible in cases of rural areas, or specific fields such as test tracks.

Various technologies are investigated for V2V communication such as GSM cellular network [17], WiFi, WIMAX, and LTE, and hybrid [18]. Choosing an effective communication infrastructure between car and drone, such as cellular, Worldwide Interoperability for Microwave Access (WIMAX), and Wi-Fi, is another communication-related issue. Some of the technologies that are widely used on drones are given in comparison in Table 1.

Table 1. Comparison of communication technologies used on swarming UAVs.

Technology	LTE [19]	WiFi [20]	ZigBee [21]
IEEE	LTE	802.11n	802.15.4
Operating Frequency	>20 MHz	2.4/5 GHz	868–915 MHz
Licensed Spectrum	Yes	No	No
Outdoor Range	100 km	250 m	10–20 m
Transfer Rate	300 Mbps	600 Mbps	200 Kbps
Latency	10 ms	<5 ms	<70 ms
Physical Infrastructure	Yes	No	No
Topology	Plan	AD Hoc, Star, Mesh, Hybrid	Mesh, Point-to-Point, Point-Multipoint

The sample use cases of these technologies are listed in Table 2. The communication range requirement depends on the bandwidth, type, length, and operating environment of the drone [15,16,21].

Table 2. Comparison of communication technologies and applications used on swarming UAVs.

Technology	Application
WiFi [20]	Emergency network establishment in disaster
LTE [22]	- Surveillance in urban areas - Expansion of coverage of the network
WiFi and ZigBee [19]	Image and data transfer in UAV network
ZigBee [23]	Cluster and swarm communication

Drones may have the functionality to follow the car similar to car-following-car. This is a well-studied field in the literature [24]. In this study, drones with the following functionality of the car under test are assumed. To simulate the following distance, test data is collected in a range of around 2 km in the field.

At ZalaZONE proving ground, a wide range of vehicle and traffic test scenarios for conventional, connected, and automated vehicles is planned to be performed [25]. Current autonomous vehicle test environments are concentrated on an urban test area for the testing and validation of connected and automated vehicles [26]. The intention is to link the drone and ground vehicle segments easily and effectively. These tests are planned to show the applicability of drone-to-car communication during car tests at the test track and potentially extend the scenario-based autonomous ground vehicle testing capabilities such as security, interaction between surrounding [27] and incorporate the unmanned aerial vehicles either in real-time testing or for real-time connection between the real world and its virtual representation [28].

Medetov et al. performed research to evaluate the energy efficient broadcast protocol in mobile ad hoc networks. As both MANET nodes and drones have limited battery capacity, efficiency of communication protocols become important for the duration of the flight. Their findings show that no protocol was superior to other by means of energy efficiency [29]. As the drones are a subject of system design, and the endurance is an input parameter in drone design, the energy requirement of the communication system will be considered in the design of drone battery.

Autonomous cars are the wave of the future in the automobile industry which seems to have both direct and indirect effects on society, economy, and environment. On one hand, autonomous cars are expected to decrease the rate of incidents and accidents by eliminating driver errors. These positive outcomes of the automated cars will potentially trigger a significant shift in the usage of the transportation mode to public and active transportation such as biking to personal or public vehicles. However, this transition will result in more emissions and greenhouse gas generations. The direct effects include resource use and emissions while the indirect effects are mainly societal such as fewer vehicles on the road, fewer vehicle miles traveled, and few CO₂ emissions [30]. With the increasing demand for environmentally friendly cars and social life quality, autonomous cars seem to form a new era. Therefore, car manufacturers, engineers, researchers, and policymakers need to address the potential negative health impacts and increase public awareness.

2. Methodology

In this research, autonomous cars under test on the test track and drones following them to collect drive data are simulated by using transmitters/receiver couples at various altitudes of 45, 95, and 165 cm. The experiments consist of the following phases which are shown in Figure 1. In the first phase, the test environment and measurement setup are designed. The antenna couples heights are selected according to vehicle height and drone flight altitude. In this phase, Low Power Long Range Transceiver (LoRa) devices are selected to be used. The spectrum analyzer and a signal generator are prepared to be used with the setup. In the second phase, the measuring devices are calibrated. During the calibration, various indoors and outdoors experiments are performed. In the third phase the data is collected in the field. In the final phase collected data are analyzed with MATLAB and curve fitting and optimization are performed.

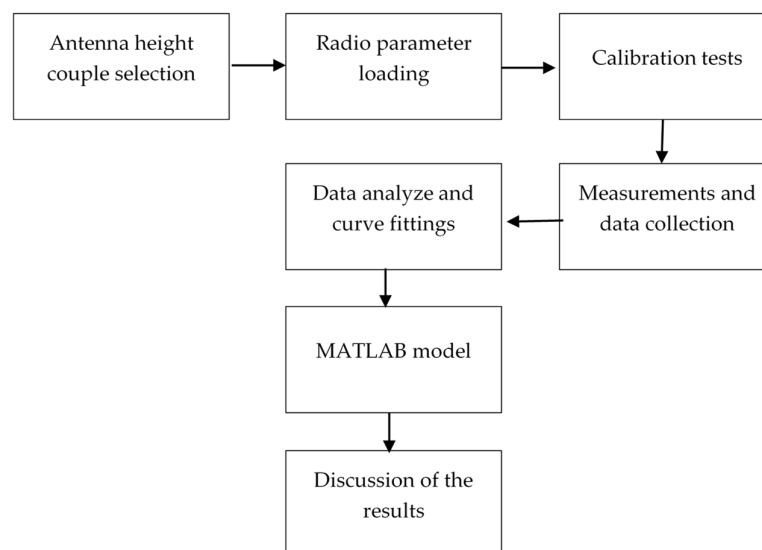


Figure 1. The experimental procedure flowchart.

LoRa is a modem with long-range spread spectrum communication capability. It also has high interference immunity with very low current consumption which makes it suitable especially for outdoor field experiments.

A Programmable Logic Controller (PLC) is used with LoRa as well. The limit of the number of data obtained with the Frequency Shift Keying (FSK) code in LoRa, and test parameters such as frequency and bandwidth are adjusted. PCBs are developed in the lab as prototypes (Figure 2). Codes are developed for data acquisition and the software is transferred to the controller PCBs which is shown in Figure 3. The transmitter and receivers are installed on wooden masts with batteries attached as shown in Figure 4.

The calibration of the system is performed by comparing the path loss measurement results with theoretical path loss equation values. Experiments in both indoor and outdoor environments are carried out to detect and/or repeat these errors. During the calibration, a setup consistent of signal generator and spectrum analyzer is used which is shown in Figure 5. The calibration measurements show that the RSSI values provided by the hardware are accurate and the resolution of the measurements is high enough to capture the 1 dB attenuation. Also, test results and the curve fitting show that the measurement capability of the test equipment used is linear throughout the power range.

The receiver's frequency, bandwidth, spreading factor, encoding rate, output power, and gain are set in the Low Noise Amplifier (LNA) LoRa Library. Some important parameters written on SemTech LoRa SX1278 are shown in Table 3.

Table 3. SEMTECH LoRa SX1278 Parameters.

Features	RF Module-1	RF Module-2
Frequency Range	820/950 MHz	868/915 MHz
Feeding Voltage	2/3.6 V	1.8/3.6 V
Modulation Technique	FSK/GFSK/OOK	FSK/GFSK/MSK/LoRa
Communication Interface	SPI	SPI
Sensitivity (Max)	−123 dBm	−139 dBm
Exit Power	16 dBm	20 dBm
Data Velocity (Max)	1.2 Mbps	300 kbps
Antenna Out	50 ohm	50 ohm

The test parameters are as follows:

- Frequency: 434 MHz, (half of the 868 MHz)
- Bandwidth: 125 kHz.
- Link spreading factor: 9.
- Output power: 17 dBm.
- The gain of the receiver LNA: 0 (automatic gain control)

The transmitter and receiver section of the test setup is shown in Figure 6. The receiver part of the antenna system with three different heights simulating altitudes of drone and car antenna positions. The minimum height of 45 cm is supposed to simulate the car antenna position and the three heights are for possible drone positions. The transmitter generates Continuous Wave (CW) signals at 868 MHz. In the receiver part, there is also a LoRa module. Omnidirectional GSM antennas with 2.5 dB gain are used for both the transmitter and receiver parts.

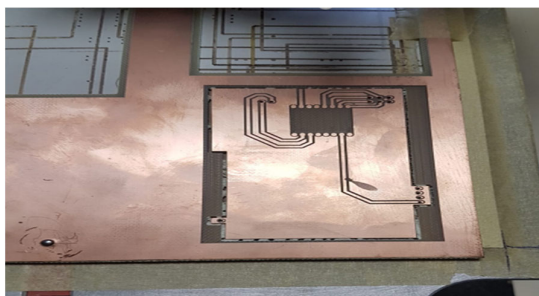


Figure 2. Lab prototype of the PCB.

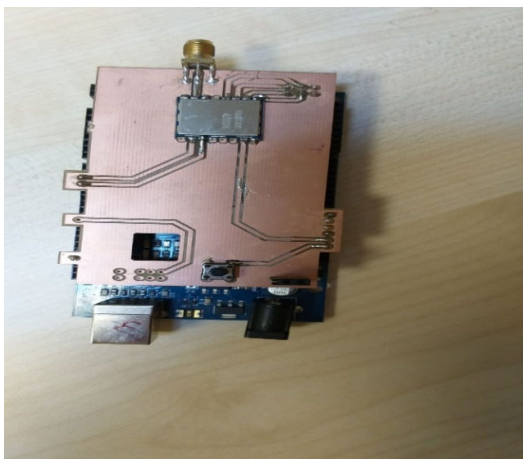


Figure 3. Codes are developed for data acquisition and the software is transferred to the controller PCBs.



Figure 4. Transmitter system with battery installed.

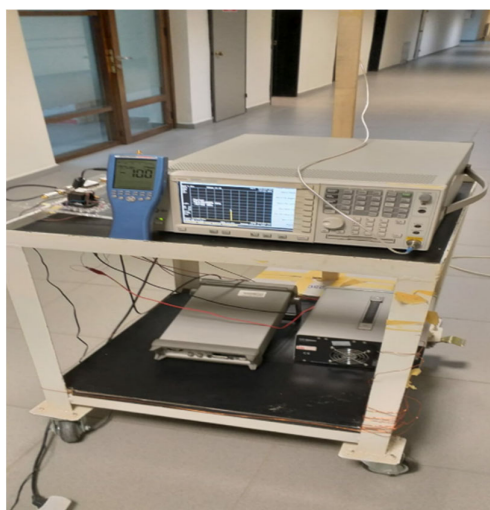


Figure 5. Calibration experiment test setup, with spectrum analyzer and signal generator.



Figure 6. Transmitter and receiver part of the measurement system, at three different heights: 45 cm, 95 cm, and 165 cm.

In 6 separate configurations (altitude couples), transmitting and receiving antenna heights are arranged. At each signal strength measuring point, all these variations are used.

A laptop is used to control the spectrum analyzer and to record the measurement data from the receiver component of LoRa systems. At each measurement point, for 6 separate antenna height combinations, around 200 measurements are recorded. The altitude combinations of antenna heights are given in Table 4.

Table 4. Antenna height combination set.

Antenna Altitude Couples	Altitude Combinations (Tx / Rx)	Color Indicated in Graph
First Combination	Tx 45 cm/Rx 45 cm	Green
Second Combination	Tx 45 cm/Rx 95 cm	Red
Third Combination	Tx 45 cm/Rx 165 cm	Blue
Fourth Combination	Tx 95 cm/Rx 95 cm	Cyan
Fifth Combination	Tx 95 cm/Rx 165 cm	Magenta
Sixth Combination	Tx 165 cm/Rx 165 cm	Black

3. Results

The test height is taken into account in calibration calculations for the change of distance surface reflections by the following equation [31]:

$$h \geq D \quad (1)$$

The overall largest antenna length (D) in the measurement system is 40 cm. Thus, the minimum height of the antenna is required to be greater than 40 cm. So, the selected heights of 45 cm, 95 cm, and 165 cm are suitable.

The link budget equation is used to check the values of the reference path loss. It contains the free space path loss. The formula used for comparison is [32]:

$$P_R(\text{dB}) = P_T(\text{dB}) - L_{\text{sys}}(\text{dB}) + 2G_A(\text{dB}) - PL_E(\text{dB}) \quad (2)$$

$$PL_T = 20 \log \frac{4\pi d_0}{\lambda} \quad (3)$$

For free space, the theoretical path loss, including the distance between the transmitter and the receiver, is PL_T . $PL_E(\text{dB})$ is the analytical loss of direction that is extracted from outdoor calculations. $L_{\text{sys}}(\text{dB})$ gives losses in the system, including LoRa devices and connectors. $P_T(\text{dB})$ is the transmitter power which is 17 dBm. $P_R(\text{dB})$ is the receiver power. G_A is the antenna gain of the transmitter and receiver and as they are equal, $2G_A$ is used. d_0 is the distance between the receiver and transmitter antennas. The signal wavelength is given as λ . The path loss is calculated in the outdoor link using combinations of antenna height (given in Table 4) and 868 MHz frequency.

Antenna heights are represented by wooden bars, which do not contain any metal parts that do not interfere with the signal. LoRa modules are connected to the top of these wooden bars. To transfer the data from each LoRa module to the laptop, a USB cable is used. The data is stored and analyzed in the computer using Tera Term Software.

The outdoor link where experiments performed in a range of approximately starting 2000 m in total. This link has three different plant species in general and bushes and forest are present at this link. There are low shrubs and tall trees. Grass and weeds are found in the area. At the time of the test, the weeds were about 12 cm long. The second plant type is bush. The average height of the bushes is 180 cm. The third plant type is tall trees that are 4–5 m apart from each other and spread throughout the field. Their heights are up to 3 m. There are also houses and containers exist in the area.

The elevation difference between the first and last points is 71 m (1095 m and 1166 m). The received power (RSSI) and elevation (meter) versus range (kilometer) graph are shown in Figure 7 with the colors given in Table 4.

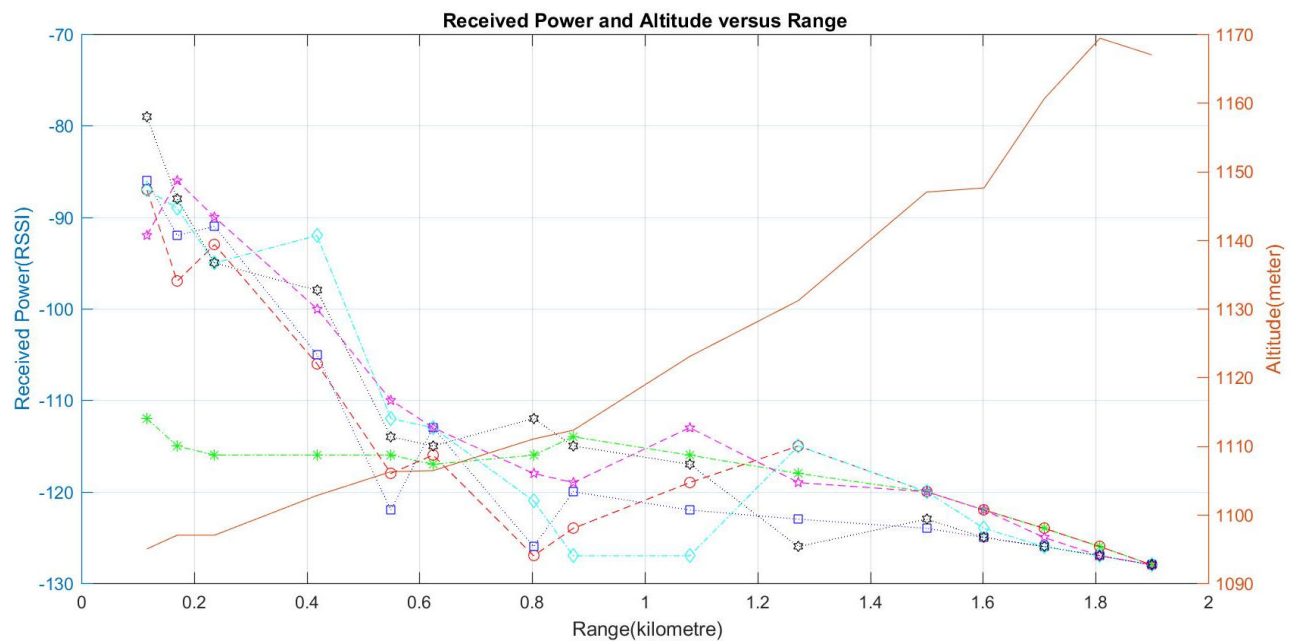


Figure 7. Received power (RSSI) values and elevation versus range on the link.

The test results are given in Table 5. The increase of the antenna height has less effect on the RSSI since the antenna height in the range of 1.5 km to 2 km in this link is lower than the plant height. When the antenna height is higher than the plant height, the effect of the antenna height on the RSSI is seen.

As antenna heights are increased, the RSSI value drops more smoothly between 0 and 1 km for the link. Since the first antenna height combination (45 cm to 45 cm) is readily influenced by human or car impacts, the RSSI value appears to change very little or not at all at the whole test range which is shown with green dots and line in Figure 2. Furthermore, this combination is made up of the antennas that are the nearest to the ground. As a result, it is susceptible to environmental factors. Hence, this part of link can act as a free space environment. Therefore, the decreasing rate of RSSI is very close to what would theoretically be expected.

The results of the test are given in Table 5. The comparison of the antenna couples is graphed in Figure 7. At the highest elevation point were also the free space environment is most closely resembled. Therefore, at this point, the rate of decrease of the RSSI approximates the theoretically expected value. On the other hand, as the elevation is increased between the receiving antenna and the transmitting antenna, the system reaches -128 dBm, the sensitivity point. As the difference in elevation increases, the signal strength of the receiving antenna reaches the sensitivity point at a shorter distance.

The path-loss depends on the distance between the vehicle and the drone. As the transmitter and receiver distance increases, the RSSI value decreases. In addition to this, as the height difference of the antennas increase, RSSI decreases.

When the receiver and transmitter antennas are both at 45 cm, the RSSI is measured as -85 dBm while they are both at 165 cm RSSI changes to -78 dBm. It is seen that when the antenna heights are increased, the ground effect decreases. After a distance, of 995 m and above, the effect of the antenna heights minimizes on RSSI value.

In Figure 8, test results are processed in MATLAB using the curve fitting method using a quadratic polynomial equation. The polynomial equation has two variables that are the logarithm of the range and receiving antenna signal strength which is plotted.

The curve fitting results for all test combinations of this link are:

- The SSE value range: 75 to 462.
- R^2 value varies between 0.75 and 0.96.
- The DFE value: 12 for all combinations.
- The Adjusted R^2 between about 0.70 and 0.96.
- RMSE between 2.50 and 6.20.
- The independent variable, called x , is normalized to an average of 6.594 for all combinations.
- The standard deviation of 0.8979 is the same for all combinations.

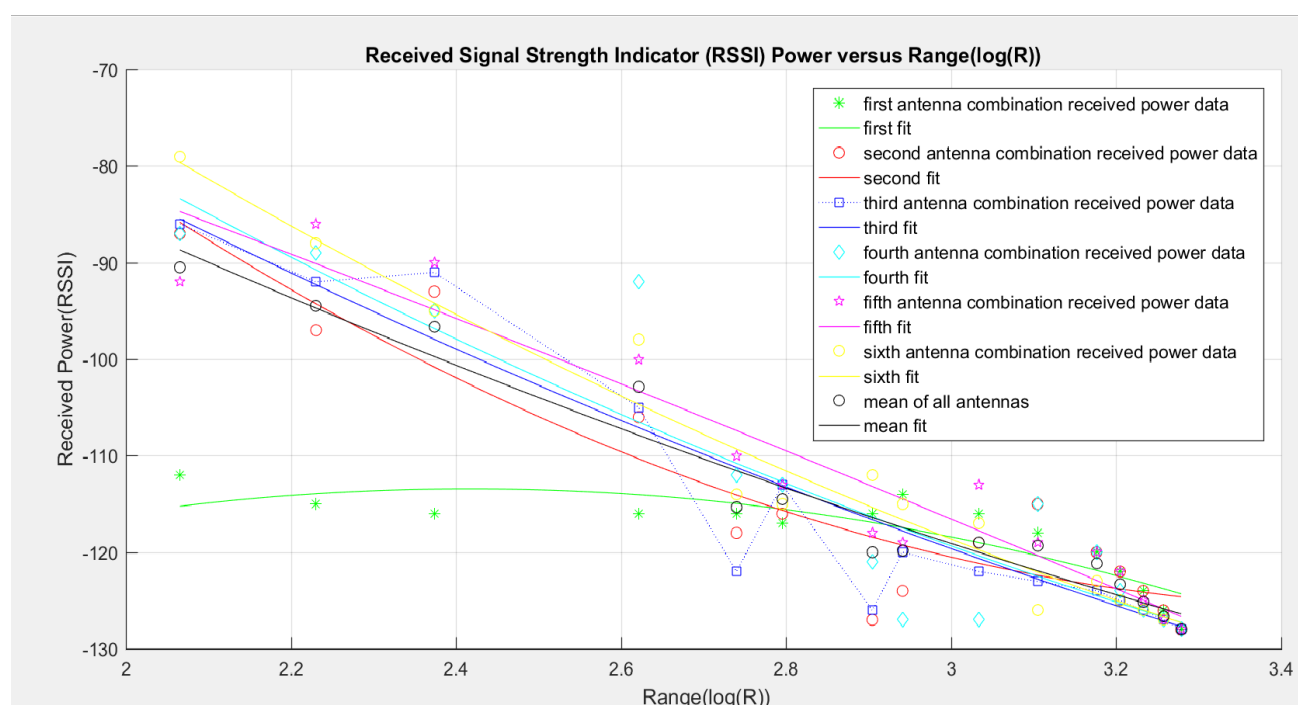


Figure 8. Curve fitting graph of the six antenna height combinations.

Figure 9 shows the curve fitting result for the average received power. The three parameters are the average receiver signal strength, the logarithm of the range value (l), and elevation value in meters (b). The average received signal strength means the average value of the receiver signal strength of all combinations at the same test point. In MATLAB, the values of x and y variables are selected to obtain the graph. The degree of x variable is selected as 2, while the value of y variable is chosen as 1. Figure 5 shows the 3D graph of the relationship between receiver signal strength, range value, and elevation values. For the MATLAB analysis, x degree 2 and y degree 1 are selected to include the terrain factor. The SSE was calculated as 79.35 and R^2 calculated as 0.9622. DFE is calculated as 10. Adjusted R^2 is found to be 0.9471 and RMSE is 2.817. The variable x is normalized to an average of 6.594 and the standard deviation is calculated as 0.8979.

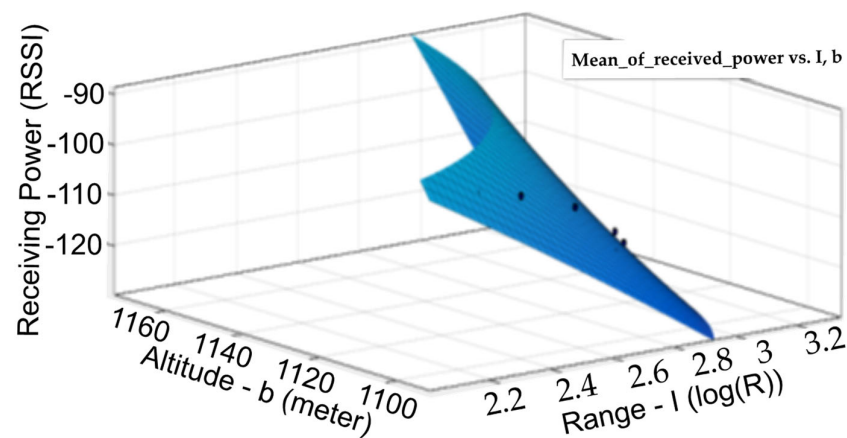


Figure 9. The curve fitting result of the first link for three parameters: Range (l) ($\log(R)$) versus mean of received power (RSSI) and elevation (b).

Table 5. Measurement point details and test results for each measurement point.

Transmitter Antenna Height (Tx cm)			45	45	45	95	95	165
Receiver Antenna Height (Rx cm)			45	95	165	95	165	165
Color on the Graphic			Green	Red	Blue	Light Blue	Purple	Black
Measurement Points	Range (Meter)	Elevation (Meter)	Receiver Signal Strength (RSSI)					
1	116.25	1095.00	−112	−87	−86	−87	−92	−79
2	170.00	1097.00	−115	−97	−92	−89	−86	−88
3	236.40	1097.00	−116	−93	−91	−95	−90	−95
4	418.09	1102.78	−116	−106	−105	−92	−100	−98
5	549.35	1106.26	−116	−118	−122	−112	−110	−114
6	624.21	1106.41	−117	−116	−113	−113	−113	−115
7	802.52	1111.02	−116	−127	−126	−121	−118	−112
8	873.09	1112.29	−114	−124	−120	−127	−119	−115
9	1079.70	1123.05	−116	−119	−122	−127	−113	−117
10	1272.53	1131.19	−118	−115	−123	−115	−119	−126
11	1500.00	1147.00	−120	−120	−124	−120	−120	−123
12	1602.08	1147.60	−122	−122	−125	−124	−122	−125
13	1708.60	1160.56	−124	−124	−126	−126	−125	−126
14	1807.78	1169.41	−126	−126	−127	−127	−127	−127
15	1899.68	1166.99	−128	−128	−128	−128	−128	−128

4. Discussions

The fact that RSSI varies with antenna height is an important aspect of this research. As a result, increasing the antenna height is essential for determining RSSI variation. Plant scattering, reflection, and diffraction impact the wireless signal in addition to ground reflection. The path loss is also decreased as the antenna height is increased.

When the results of the third antenna couple where Tx is at 45 cm and Rx is at 165 cm, are compared with other methods of the literature. The models compared are Free Space, Lee Philadelphia, Lee Newark, and Lee Tokyo. The comparison results are given in Figure 10.

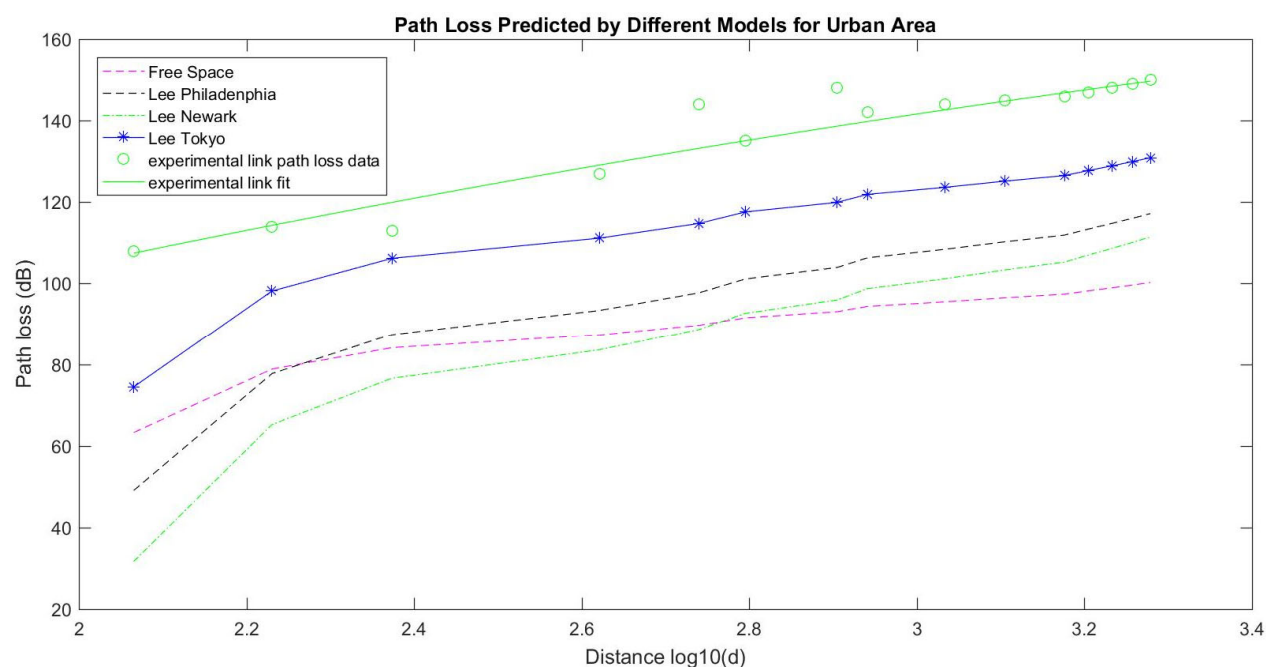


Figure 10. Comparison of the results of 45 cm Tx and 165 cm Rx test with other models.

At the distance range of 170 m to 420 m (between 2.23 and 2.62 m on the Figure 10), the Lee Tokyo model fits best for the experimental link results of the third antenna height combination. Experimentally developed model in this research has enough level of precision as shown by the graph and can be used in planning of antenna height and distance planning in track tests.

5. Conclusions

Autonomous Vehicles (AVs) will have a great role in the social life of the near future. AVs are also seen as a key for more sustainable answer for the road transport. The AVs and related technologies are currently under development and there is a need for testing AVs in the field, during operation, before the technology is accepted by the community. For the test that will be performed on test track, there are cases where ground stations can be costly and, in some cases, have technological barriers.

One of the mutual technological parts will be the communication capability which is already a reality in today's life. In this article, the Air-to-Air (A2A) and Air-to-Ground (A2G) communication channels between drones and AVs, at operating frequencies at sub-GHz, were examined. The results of the outdoor link experiments were analyzed to model the effect of distance and ground between transmitter and receiver antenna and path loss at varying altitudes of drones.

Low altitude drones can be used to collect data from the car on the test track, removing the need for a data collection infrastructure. There are several other benefits of air-to-ground communications such as removing the relative speed between the car and the drone, sending the real-time data from the car to a remote base, and video streaming/capturing at the same time.

In such low altitude applications, drone to car communication is subject to distortions such as ground effect and losses. In this research, an experimental setup is used to simulate the order of the losses of low altitude flying drones at 45 cm, 95 cm, and 165 cm. Using the collected test data, a mathematical model is developed and compared with the experimental results.

The experiment results show the effect of the ground on the communication between the car and the drone. The ground effect is very high especially on the low altitude (45 cm) tests in short-range, therefore, the RSSI figure does not change radically for long-range. Taking into account only 45 cm low altitude tests, the ground effect is constant and flat on short and long-range communication.

In this research, communication efficiency is analyzed between various antenna height/altitude combinations in a rural environment. It is shown that communication between autonomous car under track test and drones can be efficiently performed at distances up to 400 m. On longer distances, ground effect plays an important role and signal strength drops more quickly.

Research shows that if drone altitude and car antenna height are lower such as around 45 cm, RSSI decreases because of the ground effect. In a track test, drone altitude between 95 to 165 cm with antenna of the autonomous car installed at around 95 cm seems to give highest possible communication efficiency.

As a result of this experiment, researchers choose to go with 95 cm height of the car antenna and 165 cm flying altitude of drone with a maximum range (x) of 400 m between car under test and the drone as shown in the Figure 11.

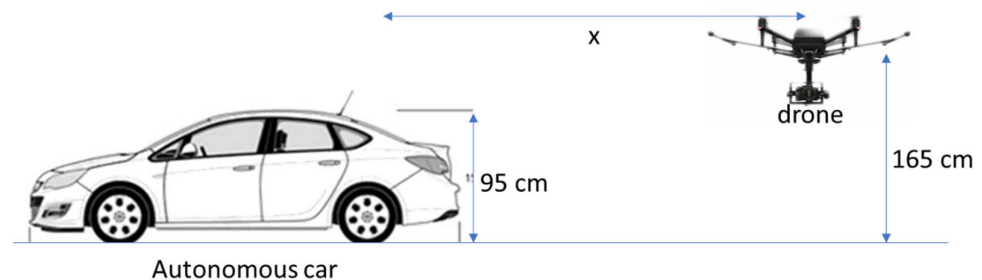


Figure 11. Optimum positioning of the drone and autonomous car. Figure shows the coupling of drone at 165 cm and car antenna at 95 cm height.

It can be concluded that the drones and cars under test can be used in conjunction, especially when the drone has the car following capability. The test results are promising, and thus might be further addressed also at ZalaZONE. The results of this research shed light on the determination of optimum range of Rx/Tx antenna height/altitude couples.

Developed path loss model can be used in a drone–car communication planning in test zones. It is shown that the accuracy of the developed model is consistent with the real environmental test results.

6. Future Work

Following the results of this research, a communication device configuration will be tested for determining further communication parameters such as packet delay and optimum bandwidth for real world application. We were seeking an answer on the possibility of the communication with the drone at a low altitude with the car under test, and if possible, to what distance the communication would be less effected by the ground effect. Thus, on further research, we plan to design a drone for the application on the autonomous car track test field. The results of this work are expected to give an insight about the range and possibility to use the drone at the low altitudes for communication. In future work, the mission specifications and duration will be an input on the sizing of the battery of the drone including the energy budget of the communication subsystem.

Author Contributions: Conceptualization, M.Y. and B.B.; methodology, M.Y.; software, B.B.; validation, U.K., D.R. and M.Y.; resources, M.Y.; data curation, B.B.; writing—original draft preparation, M.Y. and B.B.; writing—review and editing, U.K.; visualization, U.K.; supervision, D.R.; funding acquisition, D.R. All authors have read and agreed to the published version of the manuscript. All the authors listed have made a substantial, direct, and intellectual contribution to the work, and approved it for publication. All authors have read and agreed to the published version of the manuscript.

Funding: This research received no external funding.

Institutional Review Board Statement: Not applicable.

Informed Consent Statement: Not applicable.

Data Availability Statement: The data presented in this study are available on request from the corresponding author.

Conflicts of Interest: The authors declare no conflict of interest.

Acknowledgments: The current authors thank to the EFOP-3.6.1-16-2016-00014 project entitled “Investigation and development of the disruptive technologies for e-mobility and their integration into the engineering education (IDEA-E)”.

References

1. Mayor, V.; Estepa, R.; Estepa, A.; Madinabeitia, G. Deploying a Reliable UAV-Aided Communication Service in Disaster Areas. *Wirel. Commun. Mob. Comput.* **2019**, doi:10.1155/2019/7521513.
2. Seliem, H.; Ahmed, M.H.; Shahidi, R.; Shehata, M.S. Delay analysis for drone-based vehicular Ad-Hoc Networks. In Proceedings of the 2017 IEEE 28th Annual International Symposium on Personal, Indoor, and Mobile Radio Communications (PIMRC), Montreal, QC, Canada, 8–13 October 2017; pp. 1–7, doi:10.1109/PIMRC.2017.8292241.
3. Shi, W.; Zhou, H.; Li, J.; Xu, W.; Zhang, N.; Shen, X. Drone Assisted Vehicular Networks: Architecture, Challenges and Opportunities. *IEEE Netw.* **2018**, *32*, 130–137, doi:10.1109/mnet.2017.1700206.
4. Wang, X.; Fu, L.; Zhang, Y.; Gan, X.; Wang, X. VNet: An infrastructure-less UAV-assisted sparse VANET system with vehicle location prediction. *Wirel. Commun. Mob. Comput.* **2016**, *16*, 2991–3003, doi:10.1002/wcm.2727.
5. Zhou, Y.; Cheng, N.; Lu, N.; Shen, X.S. Multi-UAV-Aided Networks: Aerial-Ground Cooperative Vehicular Networking Architecture. *IEEE Veh. Technol. Mag.* **2015**, *10*, 36–44, doi:10.1109/mvt.2015.2481560.
6. Oubbati, O.S.; Lakas, A.; Lagraa, N.; Yagoubi, M.B. UVAR: An intersection UAV-assisted VANET routing protocol. In Proceedings of the 2016 IEEE Wireless Communications and Networking Conference, Doha, Qatar, 3–6 April 2016; pp. 1–6, doi:10.1109/WCNC.2016.7564747.
7. Chen, L.-W.; Tseng, Y.-C.; Syue, K.-Z. Surveillance on-the-road: Vehicular tracking and reporting by V2V communications. *Comput. Netw.* **2014**, *67*, 154–163, doi:10.1016/j.comnet.2014.03.031.
8. Abdolmaleki, M.; Masoud, N.; Yin, Y. Vehicle-to-vehicle wireless power transfer: Paving the way toward an electrified transportation system. *Transp. Res. Part C Emerg. Technol.* **2019**, *103*, 261–280, doi:10.1016/j.trc.2019.04.008.
9. Nguyen, B.C.; Tran, X.N.; Dung, L.T. On the performance of roadside unit-assisted energy harvesting full-duplex amplify-and-forward vehicle-to-vehicle relay systems. *AEU-Int. J. Electron. Commun.* **2020**, *123*, 153289, doi:10.1016/j.aue.2020.153289.
10. Al-Hourani, A.; Kandeepan, S.; Lardner, S. Optimal LAP Altitude for Maximum Coverage. *IEEE Wirel. Commun. Lett.* **2014**, *3*, 569–572, doi:10.1109/lwc.2014.2342736.
11. Meng, Y.S.; Lee, Y.H.; Ng, B.C. Empirical near ground path loss modeling in a forest at VHF and UHF bands. *IEEE Trans. Antennas Propag.* **2009**, *57*, 1461–1468, doi:10.1109/tap.2009.2016703.
12. Kurnaz, O.; Helhel, S. Near ground propagation model for pine tree forest environment. *AEU-Int. J. Electron. Commun.* **2014**, *68*, 944–950, doi:10.1016/j.aue.2014.04.019.
13. Hejselbaek, J.; Nielsen, J.O.; Fan, W.; Pedersen, G.F. Empirical Study of Near Ground Propagation in Forest Terrain for Internet-of-Things Type Device-to-Device Communication. *IEEE Access* **2018**, *6*, 54052–54063, doi:10.1109/access.2018.2871368.
14. Wu, H.; Zhang, L.; Miao, Y. The Propagation Characteristics of Radio Frequency Signals for Wireless Sensor Networks in Large-Scale Farmland. *Wirel. Pers. Commun.* **2017**, *95*, 3653–3670, doi:10.1007/s11277-017-4018-5.
15. Pojda, J.; Wolff, A.; Sbeiti, M.; Wietfeld, C. Performance analysis of mesh routing protocols for UAV swarming applications. In Proceedings of the 2011 8th International Symposium on Wireless Communication Systems, Aachen, Germany, 6–9 November 2011; pp. 317–321, doi:10.1109/ISWCS.2011.6125375.
16. Kuschnig, R.; Bettstetter, C.; *Channel Measurements over 802.11a-Based UAV-to-Ground Links*; Piscataway: NJ, USA, 2020, pp. 1280–1284.
17. Santa, J.; Gómez-Skarmeta, A.F.; Sánchez-Artigas, M. Architecture and evaluation of a unified V2V and V2I communication system based on cellular networks. *Comput. Commun.* **2008**, *31*, 2850–2861, doi:10.1016/j.comcom.2007.12.008.

18. Dey, K.C.; Rayamajhi, A.; Chowdhury, M.; Bhavsar, P.; Martin, J. Vehicle-to-vehicle (V2V) and vehicle-to-infrastructure (V2I) communication in a heterogeneous wireless network—Performance evaluation. *Transp. Res. Part C Emerg. Technol.* **2016**, *68*, 168–184, doi:10.1016/j.trc.2016.03.008.
19. Zafar, W.; Khan, B.M. A reliable, delay bounded and less complex communication protocol for multicluster FANETs. *Digit. Commun. Networks* **2017**, *3*, 30–38, doi:10.1016/j.dcan.2016.06.001.
20. Asadpour, M.; Giustiniano, D.; Hummel, K.A. From ground to aerial communication: Dissecting WLAN 802.11n for the drones. In Proceedings of the 8th ACM International Workshop on Wireless Network Testbeds, Experimental Evaluation & Characterization, Miami, FL, USA, 30 September 2013; pp. 25–32, doi:10.1145/2505469.2505472.
21. Shaikh, Z.; Baidya, S.; Levorato, M. Robust Multi-Path Communications for UAVs in the Urban IoT. In Proceedings of the 2018 IEEE International Conference on Sensing, Communication and Networking (SECON Workshops), Hong Kong, China, 11 June 2018; pp. 1–5, doi:10.1109/SECONW.2018.8396356.
22. Gomez, K.; Rasheed, T.; Reynaud, L.; Kandeepan, S.; Chavez, K.M.G. On the performance of aerial LTE base-stations for public safety and emergency recovery. In Proceedings of the 2013 IEEE Globecom Workshops (GC Wkshps), Atlanta, GA, USA, 9–13 December 2013; pp. 1391–1396, doi:10.1109/GLOCOMW.2013.6825189.
23. Motlagh, N.H.; Bagaa, M.; Taleb, T. UAV-Based IoT Platform: A Crowd Surveillance Use Case. *IEEE Commun. Mag.* **2017**, *55*, 128–134, doi:10.1109/mcom.2017.1600587cm.
24. Kuang, H.; Wang, M.-T.; Lu, F.-H.; Bai, K.-Z.; Li, X.-L. An extended car-following model considering multi-anticipative average velocity effect under V2V environment. *Phys. A Stat. Mech. Its Appl.* **2019**, *527*, 121268, doi:10.1016/j.physa.2019.121268.
25. Szalay, Z.; Tettamanti, T.; Esztergár-Kiss, D.; Varga, I.; Bartolini, C. Development of a Test Track for Driverless Cars: Vehicle Design, Track Configuration, and Liability Considerations. *Period. Polytech. Transp. Eng.* **2017**, *46*, 29, doi:10.3311/pptr.10753.
26. Szalay, Z.; Hamar, Z.; Nyerges, Á. Novel design concept for an automotive proving ground supporting multilevel CAV development. *Int. J. Veh. Des.* **2019**, *80*, 1, doi:10.1504/ijvd.2019.105061.
27. Koschuch, M.; Sebron, W.; Szalay, Z.; Torok, A.; Tschurtz, H.; Wahl, I. Safety & Security in the Context of Autonomous Driving. In Proceedings of the 2019 IEEE International Conference on Connected Vehicles and Expo (ICCVE), Graz, Austria, 4–8 November 2019; pp. 1–7, doi:10.1109/ICCVE45908.2019.8965092.
28. Szalay, Z. Next Generation X-in-the-Loop Validation Methodology for Automated Vehicle Systems. *IEEE Access* **2021**, *9*, 35616–35632, doi:10.1109/ACCESS.2021.3061732.
29. Medetov, S.; Bakhouya, M.; Gaber, J.; Wack, M. Evaluation of an energy-efficient broadcast protocol in mobile ad hoc networks. *ICT 2013* **2013**, 1–5, doi:10.1109/ictel.2013.6632108.
30. Williams, E.; Das, V.; Fisher, A. Assessing the Sustainability Implications of Autonomous Vehicles: Recommendations for Research Community Practice. *Sustainability* **2020**, *12*, 1902, doi:10.3390/su12051902.
31. Peters, L. Reviews and abstracts - IEEE standard test procedures for antennas, *IEEE Antennas Propag. Soc. Newsl.* **1981**, *23*, 28–28, doi: 10.1109/MAP.1981.27542.
32. Gay-Fernandez, J.A.; Cuinas, I. Peer to peer wireless propagation measurements and path-loss modeling in vegetated environments. *IEEE Trans. Antennas Propag.* **2013**, *61*, 3302–3311, doi:10.1109/TAP.2013.2254452.